Monatsh Chem (2009) 140:153–156
DOI 10.1007/s00706-008-0046-x

ORIGINAL PAPER

Thermal isomerization in cyclopenta[*fg*]aceanthrylene

**Svetlana Marković · Sonja Stanković ·
Slavko Radenković · Ivan Gutman**

Received: 7 August 2008 / Accepted: 13 August 2008 / Published online: 27 September 2008

Abstract Two mechanisms for the isomerization of cyclopenta[*fg*]aceanthrylene to acefluoranthene were revealed. The first pathway occurs via a cyclobutyl intermediate, whereas the second pathway involves a transition state that contains an *sp*^{3}-hybridized carbon atom. Both patterns show that the Stone-Wales rearrangement requires extremely high activation energy and indicate that the isomerization process can occur only under a drastic temperature regime.

Keywords Stone-Wales rearrangement · Density functional calculations · Electronic structure · Reaction mechanisms

Introduction

Cyclopenta-fused polycyclic aromatic compounds (CP-PAHs) are recently attracting much attention from experimental [1–4] and theoretical chemists [5–7]. One of the reasons for this lies in their important role in the processes of incomplete combustion of hydrocarbon-containing fuel sources [1, 3, 4]. Namely, among other polycyclic aromatic compounds, these are considered to be responsible for the genotoxicity of respective combustion mixtures [8–10]. It was found that certain temperature intervals permit particular isomerisation and intraconversion pathways of various CP-PAHs, whereas many other reactions do not even occur [11–18]. For example, a series of FVP experiments has been performed to prepare cyclopenta[*fg*]aceanthrylene (**1**) under various experimental conditions [11]. However, these attempts have yielded mixtures of isomeric cyclopenta[*de*]aceanthrylene (**2**) and cyclopenta[*de*]phenanthrylene (**3**). It has been suggested that **1** did form, but, due to its instability, it underwent isomerization to **2** via ethynylaceanthrylene [11]. This assumption has been recently confirmed by means of density-functional-theory-based calculations [19].

Various computational approaches have been employed to provide additional information on possible thermal rearrangement processes, involving different intraconversions of CP-PAHs, and rearrangements of ethynylarenes to CP-PAHs [12, 17–21]. Stone-Wales rearrangement, i.e., the isomerisation followed with the simultaneous rearrangement of two carbon atoms, has been widely discussed [22–25]. The Stone-Wales transformation has originally been suggested as a hypothetical mechanism useful for deriving fullerene isomers [26]. Scott et al. [27] have claimed that pyracylene does not rearrange according to the Stone-Wales pathway at 1,100 °C. On the other hand, Nimlos et al. [22] have proposed two mechanisms for the Stone-Wales rearrangement of pyracylene. The first mechanism occurs via a cyclobutyl intermediate, and the second contains one transition state with an *sp*^{3}-hybridized carbon atom. The aim of this paper is to examine the possibility of extending the application of pyracylene-type rearrangement to the isomerization of **1** to acefluoranthene (**4**). Our investigation is also inspired by the work of Scott et al. [11], who tried to obtain **4** from **1** using various experimental methods. The present study rationalizes the instability and fast intraconversion of **1** and thus supports previous experimental investigations.

S. Marković (✉) · S. Stanković · S. Radenković · I. Gutman
Faculty of Science, University of Kragujevac,
34000 Kragujevac, Serbia
e-mail: mark@kg.ac.yu

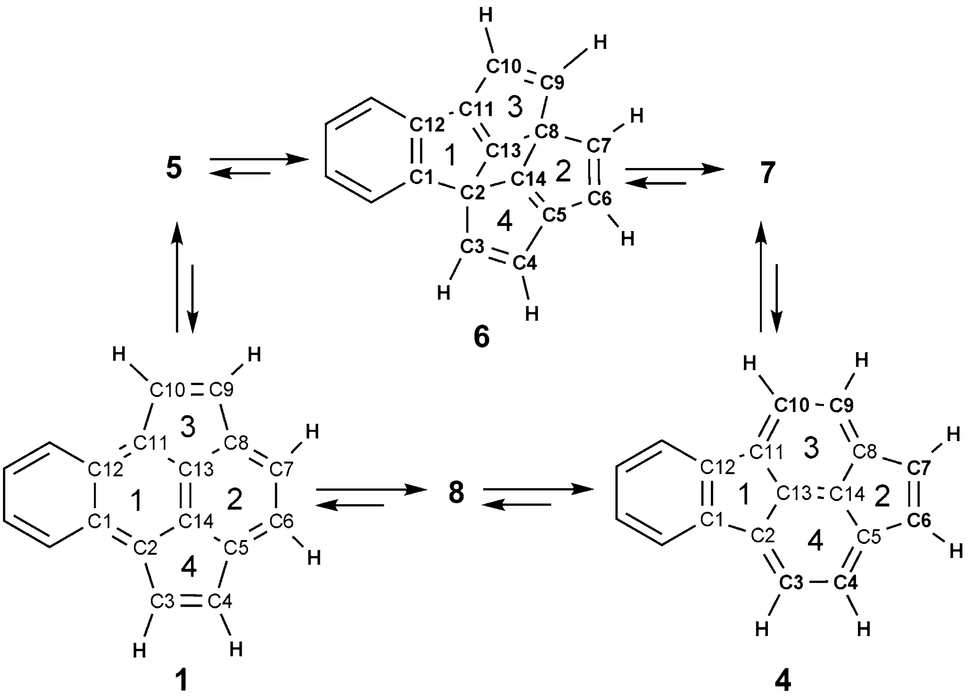

Fig. 1 Reaction scheme for two isomerization processes of **1**–**4**

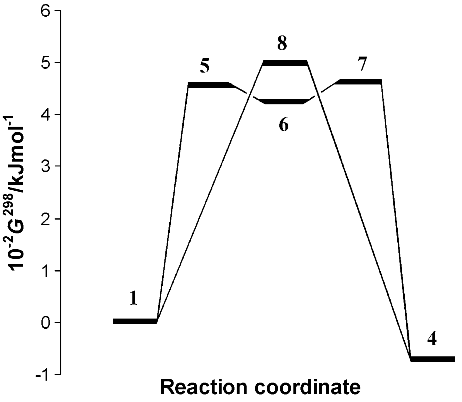

Fig. 2 Energy diagram for pathways A (**1**, **5**, **6**, **7**, **4**) and B (**1**, **8**, **4**)

Results and discussion

Our recent study [19] has shown that **1**, **2**, and **3** can undergo different intraconversion patterns for mutual isomerizations. It has been confirmed that ethynylaceanthrylene forms during the flash vacuum pyrolisis experiments, but, due to the high temperature conditions (900 °C), it transforms to either **1** or **2**. When formed, **1** surmounts the activation barrier (383.5 kJ/mol, calculated at the level of theory used in this work) and rapidly returns to **2**. Under the conditions of extreme temperature (1,100 °C), **2** and **3** undergo mutual isomerization, overcoming the high-energy barrier (383.2 kJ/mol) and forming the isomeric mixture.

This paper examines possible reaction paths for the Stone-Wales rearrangement of **1**. Two mechanisms for the isomerization of **1** to **4** were revealed: pathway A occurs via the transition states **5** and **7**, and the cyclobutyl intermediate **6**, whereas pathway B involves a transition state **8** that contains an sp^3-hybridized carbon atom (Fig. 1).

The energetic diagram of the reactions is depicted in Fig. 2. The optimized geometries of all transition states are presented in Fig. 3. Compounds **1** and **4** are planar molecules, whereas the planarity in **5**–**8** is significantly disturbed. The bond lengths of all intermediates and transition states are given in Table 1, whereas the values of the total energies, enthalpies, and free energies are provided in Table 2.

A cleavage of the double C13–C14 bond of **1**, followed by the simultaneous formation of the C2–C13 and C8–C14 bonds, is considered as the first step in pathway A. A transition state **5**, which requires an activation energy of 458.2 kJ/mol, is revealed. Here, a weak σ(C2–C13) bond with the hybrid composition $0.71(sp^{5.01})_{C2} + 0.70(sp^{2.21})_{C13}$ is observed. Thus, the six-membered ring 1 of **1** has contracted into a five-membered ring, whereas ring 2 has extended into a seven-membered ring (Fig. 3). By the formation of the C8–C14 bond, the transition state **5** is stabilized, yielding the intermediate **6**. Here, rings 1–4 are all five-membered, and there is a four-membered cycle between rings 1 and 2 (Fig. 1). The maps of the HOMO and LUMO in **6** are presented in Fig. 4. The HOMO and LUMO maps delineate the areas that are most electron-sufficient (C13 and C11) and electron-deficient (C14). Following this consideration, we examined the formation of the C13–C14 bond as the second step of pathway A.

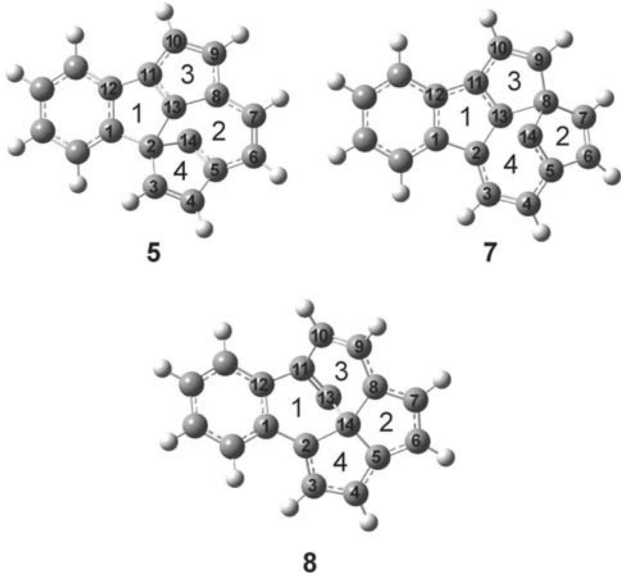

Fig. 3 Optimized geometries of all transition states in the two isomerization processes of **1**

Table 1 Selected bond distances/pm in the intermediates and transition states in the isomerization processes of **1**

	1	4	5	6	7	8
C1–C2	141.6	148.9	150.0	150.3	145.2	146.5
C1–C12	148.7	144.0	141.7	146.1	143.1	142.4
C2–C3	149.1	139.0	145.6	149.2	142.6	141.6
C2–C13	242.3	140.9	159.2	156.3	149.9	202.6
C2–C14	138.9	242.5	149.5	156.1	210.6	153.9
C3–C4	136.7	144.4	136.1	136.7	135.7	139.9
C4–C5	148.9	139.1	145.4	145.2	142.4	140.7
C5–C6	138.3	148.5	143.2	145.2	145.7	140.2
C5–C14	141.5	140.7	140.8	139.3	141.3	147.1
C6–C7	145.8	136.9	136.5	135.6	136.0	140.4
C7–C8	138.3	148.5	144.4	149.1	148.6	140.7
C8–C9	148.9	139.1	143.8	149.0	149.4	143.5
C8–C13	141.5	243.1	150.9	156.6	162.2	208.9
C8–C14	243.8	140.7	199.7	157.7	148.3	157.5
C9–C10	136.7	144.4	138.3	135.7	135.6	137.4
C10–C11	149.1	139.0	142.3	145.1	144.7	144.8
C11–C12	141.6	148.9	145.4	146.1	143.8	147.4
C11–C13	138.9	140.9	140.2	138.7	139.5	137.3
C13–C14	136.7	135.9	169.4	184.2	168.1	145.2

Table 2 Total energies (E), enthalpies (H^{298}), and free energies (G^{298}) for all participants in the reactions

Species	E/kJ mol^{-1}	H^{298}/kJ mol^{-1}	G^{298}/kJ mol^{-1}
5	456.7	455.8	458.2
6	422.4	421.9	423.8
7	480.6	480.2	481.6
8	500.6	500.7	501.1
4	−70.5	−70.9	−70.3

The energies are calculated relative to **1**

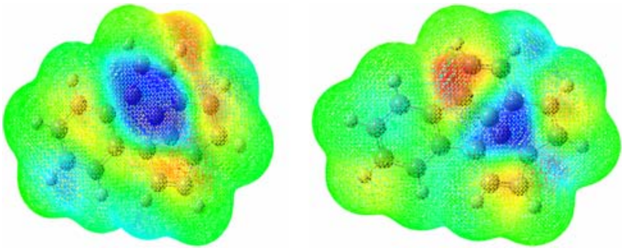

Fig. 4 HOMO (*left*) and LUMO (*right*) map of **6**. The regions where the values of the orbitals are greatest are indicated in *blue*, whereas the regions where they are least are indicated in *red*

The transition state **7** is obtained (Fig. 3), requiring an activation barrier of 57.8 kJ/mol. Here, the C8–C13 bond is elongated, the C2–C14 bond is broken, and the C13–C14 bond is being formed (Table 1, Fig. 3). The hybrid composition of the C8–C13 bond [$0.71(sp^{5.57})_{\mathrm{C8}} + 0.71(sp^{2.25})_{\mathrm{C13}}$] is in agreement with its length. Thus, cycle 4 has become a seven-membered ring. Further changes in **7** (i.e., the cleavage of the C8–C13 bond and the formation of the C13–C14 bond) lead to the formation of the product **4**.

In pathway B a shift of the π(C13–C14) to the position 11–13 is considered as a plausible one-step isomerization process. The transition state **8**, requiring an activation energy of 501.1 kJ/mol, is found out (Fig. 3). The C8–C13 bond is being broken, the C2–C13 bond is being formed, and a weak σ(C8–C14) bond with the hybrid composition of $0.69(sp^{2.8})_{\mathrm{C8}} + 0.72(sp^{2.72})_{\mathrm{C14}}$ is formed. The six-membered rings 1 and 3 are significantly deformed, and the C13 atom is approximately *sp* hybridized. As the C8–C13 bond is completely broken and the C2–C14 bond is formed, the product **4** is obtained.

The results of the IRC calculations for the transition states **7** and **8** are presented in Fig. 5.

Figure 2 and Table 2 show that the Stone-Wales rearrangement requires an extremely high activation energy. The rate determining steps for pathways A and B amount to 481.6 and 501.1 kJ/mol. These mutually similar activation barriers are even higher than those observed in the thermal conversions of **1**–**2** and **2**–**3**. These facts indicate that both isomerization processes can occur only under drastic temperature conditions. We suppose that this temperature is higher than 1,100 °C, i.e., the temperature under which the isomerization between **2** and **3** occurs.

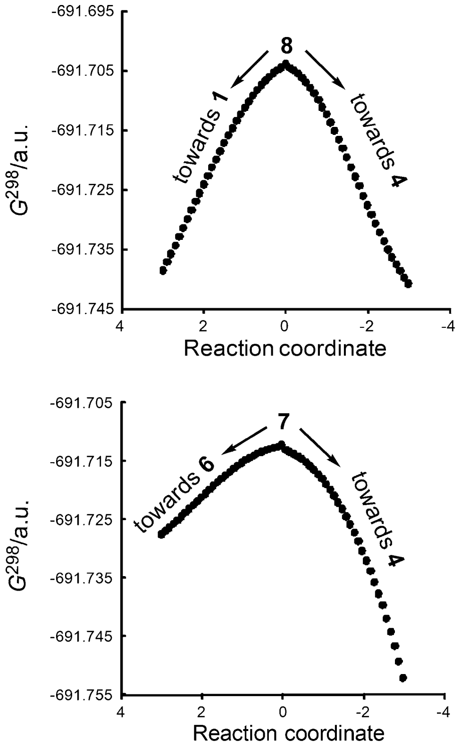

Fig. 5 Results of the IRC calculations for the transition states **7** and **8**

Methods

All calculations were conducted using Gaussian 03 [28] with the B3LYP hybrid functional [29–31]. The split valence basis set 6-31G(d) was used. This polarized basis set adds d functions on heavy atoms. The suitability of this level of theory for studies of reactions involving arenes and carbenes has been previously established [22, 24, 32]. Geometric parameters of all investigated species were optimized in vacuum. Vibrational analysis and natural bond orbital (NBO) [33] analysis were performed for all structures. All calculated structures were verified to be local minima (all positive eigenvalues) for ground state structures or first-order saddle points (one negative eigenvalue) for transition state structures by frequency calculations. From the transition structures, the intrinsic reaction coordinates (IRCs) were obtained using the IRC routine in Gaussian.

Acknowledgments This work is supported by the Ministry of Science of Serbia, project no. 144015G and 142025.

References

1. Luthe G, Wiersum UE, Brinkman UAT (2005) Polycycl Aromat Compd 25:95
2. Marsh ND, Ledesma EB, Wornat MJ, Tan MP, Zhu D, Law CK (2005) Polycycl Aromat Compd 25:227
3. Devos O, Combet E, Tassel P, Paturel L (2006) Polycycl Aromat Compd 26:69
4. Duedahl-Olesen L, White S, Binderup ML (2006) Polycycl Aromat Compd 26:163
5. Gutman I, Furtula B (2008) Polycycl Aromat Compd 28:136
6. Gutman I, Đurđević J (2008) MATCH Commun Math Comput Chem 60:659
7. Gutman I, Đurđević J, Furtula B, Milivojević B (2008) Indian J Chem 47A:803
8. Otero-Lobato MJ, Kaats-Richters VEM, Havenith RWA, Jenneskens LW, Seinen W (2004) Mutat Res 564:39
9. Wang J, He X, Mulder PPJ, Boere BB, Cornelisse J, Lugtenburg J, Busby WFJ (1999) Carcinogenesis 20:1137
10. Howard JB, Longwell JP, Marr JA, Pope CJ (1995) Combust Flame 101:262
11. Scott LT, Necula A (1997) Tetrahedron Lett 38:1877
12. Sarobe M, Jenneskens LW, Wesseling J, Snoeijer JD, Zwikker JW, Wiersum UE (1997) Liebigs Ann/Recueil 1207
13. Sarobe M, Kwint HC, Fleer T, Havenith RWA, Jenneskens LW, Vlietstra EJ, van Lenthe JH, Wesseling J (1999) Eur J Org Chem 1191
14. Necula A, Scott LT (2000) J Anal Pyrol 54:65
15. Jenneskens LW, Sarobe M, Zwikker JW (1996) Pure Appl Chem 68:219
16. Scott LT, Roelofs NH (1987) J Am Chem Soc 109:5461
17. Sarobe M, Jenneskens LW, Wesseling J, Wiersum UE (1997) J Chem Soc Perkin Trans 2:703
18. Marsh ND, Wornat MJ (2004) J Phys Chem 108:5399
19. Marković S, Stanković S, Radenković S, Gutman I (2008) J Chem Inf Model (in press)
20. Cioslowsky J, Schimeczek M, Piskorz P, Moncrieff D (1999) J Am Chem Soc 121:3773
21. Violi A, Sarofim AF, Truong TN (2001) Combust Flame 126:1506
22. Nimlos MR, Filley J, McKinnon JT (2005) J Phys Chem 109:9896
23. Balaban AT, Schmalz TG, Zhu H, Klein DJ (1996) J Mol Struct Theochem 363:291
24. Alder RW, Harvey J (2004) J Am Chem Soc 126:2490
25. Scott LT (1996) Pure Appl Chem 68:291
26. Stone AJ, Wales DJ (1986) Chem Phys Lett 129:501
27. Scott LT, Warren HB (1992) In: Seventh international symposium on novel aromatic compounds. Victoria, BC, Canada, abstr. no. 65
28. Frisch MJ, Trucks GW, Schlegel HB, Scuseria GE, Robb MA, Cheeseman JR, Zakrzewski VG, Montgomery JA Jr, Stratmann RE, Burant JC, Dapprich S, Millam JM, Daniels AD, Kudin KN, Strain MC, Farkas O, Tomasi J, Barone V, Cossi M, Cammi R, Mennucci B, Pomelli C, Adamo C, Clifford S, Ochterski J, Petersson GA, Ayala PY, Cui Q, Morokuma K, Malick AD, Rabuck KD, Raghavachari K, Foresman JB, Cioslowski J, Ortiz JV, Baboul AG, Stefanov BB, Liu G, Liashenko A, Piskorz P, Komaromi I, Gomperts R, Martin RL, Fox DJ, Keith T, Al-Laham MA, Peng CY, Nanayakkara A, Challacombe M, Gill PMW, Johnson B, Chen W, Wong MW, Andres JL, Gonzalez C, Head-Gordon M, Replogle ES, Pople JA (2003) Gaussian 03, Revision E.01-SMP, Gaussian Inc., Pittsburgh
29. Becke AD (1988) Phys Rev A 38:3098
30. Lee C, Yang W, Parr RG (1988) Phys Rev B 37:785
31. Becke AD (1993) J Chem Phys 98:5648
32. Bettinger H, Yakobson BI, Scuseria GE (2003) J Am Chem Soc 125:5572
33. Weinhold F, Landis CR (2005) Valency and bonding: a natural bond orbital donor–acceptor perspective. Cambridge University Press, Cambridge